

Characterizing Wideband Signal Envelope Fading in Urban Microcells Using the Rice and Nakagami Distributions

Gregor Gaertner and Eamonn O Nuallain

Abstract—In this paper, we show that the cumulative and probability distribution functions (cdf and pdf, respectively) of small-scale wideband signal envelope fading in microcells can be very closely approximated by both the Rice and Nakagami distributions, which are already known to describe the cdfs and pdfs of small-scale narrowband signal envelope fading. Our results are obtained by means of an extensive Monte Carlo-based study of a wideband propagation model by Yan and Kozono, which is itself supported by extensive measurements. Over a comprehensive range of microcell propagation parameters, the average maximum error in the approximation is 1.65% and 1.78% for the Rice and Nakagami cdfs, respectively. The error in the approximation is 3.58% and 3.87% for the 95th percentile and does not exceed 7.61% and 7.80%, respectively, in the worst case. We propose an expression that maps the significant wideband small-scale signal envelope fading parameters to their narrowband counterparts for different standards like Dedicated Short Range Communication, WiMAX, Universal Mobile Telecommunications Service, and the family of the IEEE 802.11 standards. This mapping enables narrowband small-scale signal envelope fading statistical distributions, which are currently used, e.g., in fading simulators, link quality determination algorithms, and outage probability calculators, to be readily adapted to deal with small-scale wideband signal envelope fading. As an application example of this proposed mapping, we derive the appropriate sample spacing and averaging interval (window size) that ought to be used to estimate the large-scale fading signal in an IEEE 802.11 receiver.

Index Terms—Broadband communication, fading channels, simulation, statistics.

I. INTRODUCTION

WITH THE proliferation of laptop/palmtop computers and computationally powerful mobile phones, there has been a growing demand for high-quality mobile multimedia services. Such services are being increasingly offered in urban microcellular environments. At the physical layer, good quality service is synonymous with reliable transmission with high data throughput, with the latter necessitating a wideband signal. In general, the wideband signal envelope shows less severe small-scale and short-term fading [2] than the narrowband signal envelope. The reason for this is that wideband signals inherently exploit frequency diversity [2]–[4]. Although the probability

distributions of small-scale narrowband signal envelope fading have been extensively studied, e.g., in [5]–[9], for which closed-form expressions exist, comparatively few such studies are reported for wideband systems [1], [3], [4], [10], and closed-form expressions for the cumulative distribution function (cdf) and probability distribution function (pdf) of the small-scale fading envelope are unavailable.

Our motivation to investigate this topic stemmed from our study of link quality prediction in an IEEE 802.11 urban microcellular system [11]. This paper suggested that link quality prediction may significantly benefit from the incorporation of wideband signal envelope fading statistics when estimating the outage probability.

In the literature, Yan and Kozono [1], [3] have proposed a wideband signal propagation model with which they investigated the properties of the received signal envelope of a mobile receiver. They verified their model with extensive measurements performed in the Tokyo region and observed that the fading depth is strongly dependent not only on the ratio of the direct to indirect power of the wideband signal but also on what they term the “equivalent received bandwidth,” which is the product of the receiver bandwidth and the maximum difference in propagation path lengths. They also observed that the distribution of the signal envelope is almost independent of the carrier frequency. Their results also demonstrate that wideband signals, in general, exhibit shallower fades than narrowband signals and that small-scale wideband signal envelope fading in non-line-of-sight (NLOS) conditions cannot, in general, be characterized using the Rayleigh distribution. They did not investigate, however, whether other known distributions can do this. Similar results to those given above were reported by Yamaguchi *et al.* [4].

Oh *et al.* [10] have shown that the distribution of the small-scale code-division multiple-access signal envelope can be described using the Nakagami distribution. Although this latter study is limited to only two receiver bandwidths deployed in two types of urban environment, namely, urban high rise and urban residential, they suggested to us the possibility that the Nakagami and the closely related Rice distribution could be used as a general means with which to describe the distribution of the small-scale fading wideband signal envelope, albeit to a certain degree of approximation. Yan and Kozono’s observation that the fading depth in a wideband signal is strongly dependent on both the ratio of the direct to indirect power (or “wideband power ratio”) and the “equivalent received bandwidth” suggests

Manuscript received April 11, 2006; revised November 25, 2006 and January 21, 2007. The review of this paper was coordinated by Prof. A. Abdi.

The authors are with the Distributed Systems Group, Department of Computer Science, Trinity College Dublin, Dublin 2, Ireland (e-mail: gregor.gaertner@cs.tcd.ie; eamonn.nuallain@cs.tcd.ie).

Digital Object Identifier 10.1109/TVT.2007.901857

the possibility of mapping these to the Ricean K -factor and the approximately related Nakagami shape factor “ m ,” thus providing a means to accurately describe the distribution of the small-scale fading wideband signal envelope using the classical narrowband distributions. We henceforth refer to the equivalent received bandwidth and the wideband power ratio as the “wideband propagation parameters” and the Ricean K -factor and the Nakagami shape factor “ m ” as the “narrowband propagation parameters.” This paper uses a simulation and curve-fitting approach based on Yan and Kozono’s [1], [3] wideband propagation model, which is supported by extensive measurement data, to determine the distributions of the small-scale fading wideband signal envelope over a comprehensive range of urban propagation environments and receiver bandwidths. Our results show that the cdf and pdf of wideband fading signals in urban microcells can be closely approximated by the Rice and Nakagami distributions. The error in the approximation is shown to be small. We then provide an expression that maps the wideband propagation parameters to their narrowband counterparts, depending on which of the two distributions one wishes to use. This mapping allows propagation modeling and signal analysis techniques that make use of these classical small-scale narrowband fading distributions to be readily adapted to deal with wideband fading.

This paper is organized as follows. In Section II, we explain the methodology used in this paper. Following this, we evaluate the goodness-of-fit of the Rice and Nakagami distributions to the small-scale fading of the wideband signal envelope and power. In Section III, we introduce an expression that maps the wideband propagation parameters to their narrowband counterparts and apply this mapping for microcellular Universal Mobile Telecommunications Service (UMTS), Dedicated Short Range Communication (DSRC), WiMAX, and IEEE 802.11 systems. In Section IV, we present a step-by-step description of how our findings can be used to adapt narrowband solutions for wideband systems. In particular, we show in Section IV-A how to better estimate the local mean signal power in an IEEE 802.11 system. In Section IV-B, we use our results to adapt a packet-level wireless network simulation software to generate wideband small-scale signal envelope fading. Furthermore, we modify a widely used bit error probability (BEP) model for differential quadrature phase-shift keying (DQPSK) receivers in narrowband channels to model IEEE 802.11 receivers with perfect channel equalization in wideband channels. This paper concludes in Section V.

II. CHARACTERIZING THE DISTRIBUTION OF THE SMALL-SCALE FADING OF THE WIDEBAND SIGNAL ENVELOPE

It is generally accepted that the wideband propagation channel is well modeled using a tapped delay line as first proposed by Turin *et al.* [12] for an urban propagation environment. The amplitudes, phases, and time delays of the resolvable paths are usually determined by empirical measurements (see [12]–[16] for examples). However, these quasi-empirical models’ core parameters are necessarily phenomenological, and therefore, their applicability is sometimes questionable [17]. We therefore

selected, for the purposes of this paper, the wideband propagation model of Yan and Kozono [1], [3], who base their work on that of Clarke [8]. The results given by this model have been shown to correspond well with an extensive range of measurements [1], [3], [18], [19]. We therefore conclude that this model, being both robust and reliable, is a suitable model on which to base this paper.

Yan and Kozono’s [1], [3] model assumes that N multipath waves arrive at the receiver under the following conditions: each wave has an amplitude A_i , a path length L_i , and an angle of arrival θ_i . A_i and L_i are independent of each other and are uniformly distributed over a given range. θ_i is uniformly distributed over 2π in the horizontal plane. A_0 and L_0 denote the amplitude and path length of the line-of-sight (LOS) wave. The ratio of the direct to indirect power is defined as

$$a = A_0^2 / \sum_{i=1}^{N-1} A_i^2 \quad (1)$$

giving $a_{(\text{dB})}$, where

$$a_{(\text{dB})} = 10 \log a. \quad (2)$$

The bandwidth of each arriving wave, which is assumed to have a flat power spectral density, is taken to be greater than the receiver bandwidth $2\Delta f$. The received signal power α^2 (in watts) is then expressed by Yan and Kozono as follows [1, eq. (2)]:

$$\alpha^2(2\Delta f) = 2\Delta f \left(\sum_{i=0}^{N-1} A_i^2 + \underbrace{\sum_{i=0}^{N-1} \sum_{j=0}^{N-1} \frac{A_i A_j}{c}}_{i \neq j} \frac{2\pi}{c} \Delta f \Delta L_{ij} \right) \times \cos \left(\frac{2\pi}{c} f_c \Delta L_{ij} \right) \sin \left(\frac{2\pi}{c} \Delta f \Delta L_{ij} \right) \quad (3)$$

where ΔL_{ij} is the difference in the path lengths of the i th and j th arriving waves. As mentioned earlier, Yan and Kozono also propose a propagation parameter termed the “equivalent received bandwidth,” which can be used to estimate the fading depth [20]. The equivalent received bandwidth is the product of the receiver bandwidth $2\Delta f$ and the maximum difference in path lengths ΔL_{\max} of the arriving waves (i.e., $\Delta L_{\max} = \max |L_i - L_j|$). In summary, the equivalent bandwidth and, hence, the observed fading depth are dependent on the receiver bandwidth and the propagation environment.

Using Yan and Kozono’s model, we generate 10^4 samples, as suggested in [20], for each propagation environment and receiver parameter tuple $(2\Delta f, \Delta L_{\max}, a_{(\text{dB})}) \in \mathcal{S}_{2\Delta f} \times \mathcal{S}_{\Delta L_{\max}} \times \mathcal{S}_{a_{(\text{dB})}}$. Since each tuple is dependent on properties of both the receiver and the propagation environment, we refer to each tuple $(2\Delta f, \Delta L_{\max}, a_{(\text{dB})})$ as a “configuration.” Due to the very large number of sample points taken, we expect the empirical distribution function (EDF) will resemble the unknown exact cdf closely.

We chose the wideband power ratio $a_{(\text{dB})}$ to range from $-\infty$ dB (NLOS) to +15 dB (strong LOS). This range was

TABLE I
PARAMETER VALUES USED IN SIMULATIONS

Parameter	Values
$a_{(\text{dB})}$ (dB)	$\{-\infty\} \cup [1, 15]_{\text{step}=2} = \mathcal{S}_{a_{(\text{dB})}}$
ΔL_{max} (m)	$\{[0.1, 1] \cup [5, 55]_{\text{step}=5}\} = \mathcal{S}_{\Delta L_{\text{max}}}$
$2\Delta f$ (MHz)	$\{[2, 34]_{\text{step}=2}\} = \mathcal{S}_{2\Delta f}$
Number of sample points per configuration	10,000
N	10
f_c (MHz)	2442

determined to be appropriate for microcellular environments in a major empirical study [21]. The receiver bandwidth is chosen to range from 2 to 34 MHz so that the results generated here will apply to current wideband standards such as DSRC, WiMAX, UMTS, and the family of IEEE 802.11 standards. The maximum difference in propagation path lengths is estimated to range from 0.1 to 55 m based on the Cardoso and Correia [20] model for urban microcells.

All data were generated using the IEEE 802.11 center frequency f_c of 2442 MHz. Kozono [3] has reported that the statistical distribution of a fading signal is practically independent of the center frequency, and therefore, the inferences made regarding the distribution of this data will have general applicability for other wideband standards. As observed by Yan and Kozono [1], the fading depth is practically independent of the number of arriving waves for $N > 6$. As suggested by Yan and Kozono [1], we use $N = 10$ for the purposes of this paper. The list of parameters over which the data is generated is summarized in Table I.

Various hypothesis tests and criteria are given in the literature to evaluate the goodness-of-fit of an EDF to a proposed cdf. It is important to note at this stage that if a hypothesis test indicates that a fading signal is not a strict realization of the distribution under test, good agreement can, however, be of significant practical value. For this reason, we use the Kolmogorov–Smirnov (KS) test [22, vol. 4, pp. 393–396 and 398–402] throughout this paper since this test statistic enables both hypothesis testing and easily comprehensible goodness-of-fit analysis where no strict realization of the proposed cdf is given. The KS statistic gives the maximum error between the EDF and the proposed cdf.

The two-sided KS statistic for a data set $\mathcal{X} \subset \mathbb{R}$ is given by

$$\varepsilon_{\text{KS}} = \sup_{x \in \mathcal{X}} |P_{\text{EDF}}(x) - P_{\text{proposed}}(x|\Theta)| \quad (4)$$

where $P_{\text{EDF}}(x)$ is the EDF of the fading signal, and $P_{\text{proposed}}(x)$ is the proposed theoretical distribution. Θ is the Ricean K -factor or Nakagami shape factor, depending on which distribution is being used, i.e., $\Theta \in \{K, m\}$.

Throughout this paper, we also make use of the root-mean-square (rms) error

$$\varepsilon_{\text{rms}} = \sqrt{\frac{\sum_{i=1}^{|\mathcal{X}|} (P_{\text{EDF}}(x_i) - P_{\text{proposed}}(x_i|\Theta))^2}{|\mathcal{X}|}}, \quad x_i \in \mathcal{X}. \quad (5)$$

We use ε_{KS} for the formal goodness-of-fit tests and both ε_{KS} and ε_{rms} in the subsequent analysis and discussion.

Both error statistics are computed for each configuration ($2\Delta f, \Delta L_{\text{max}}, a_{(\text{dB})}$). For better readability, we express all error statistics—which are probabilities in this case—as percentages via multiplication by 100. In this way, e.g., a certain event occurs in 100% of all trials and, therefore, has a probability percentage of 100%.

The parameter Θ is obtained by means of a maximum-likelihood estimation (MLE) [22, vol. 5, pp. 341–351]. The method of moments [22, vol. 5, pp. 467–473] is used to obtain the starting points for the MLE using the simplex search method of Lagarias *et al.* [23].

The following steps are taken to obtain the error data for each configuration ($2\Delta f, \Delta L_{\text{max}}, a_{(\text{dB})}$):

- 1) generation of signal envelope/power samples using Yan and Kozono's [1], [3] model;
- 2) determination of the EDF of the signal envelope/power from the data obtained in step 1);
- 3) MLE of the parameter Θ for the Rice/noncentral chi-square and Nakagami/Gamma distributions;
- 4) establishment, using the KS test, of the formal goodness-of-fit between the proposed distributions using the parameter obtained in step 3) and the EDF obtained in step 2);
- 5) calculation of ε_{KS} and ε_{rms} using the data obtained in steps 2)–4).

A. Distribution of the Signal Envelope and Power

In this section, we evaluate the goodness-of-fit of the Rice/Nakagami distributions to the EDF of the wideband signal envelope α over the range of propagation and receiver parameter configurations $\mathcal{S}_{2\Delta f} \times \mathcal{S}_{\Delta L_{\text{max}}} \times \mathcal{S}_{a_{(\text{dB})}}$ given in Table I. The Rice distribution [24] is given as follows [25, pp. 51–53]:

$$p_{\alpha}(x) = \frac{2x(K+1)}{\Omega_p} \exp\left(-K - \frac{(K+1)x^2}{\Omega_p}\right) \times I_0\left(2x\sqrt{\frac{K(K+1)}{\Omega_p}}\right), \quad x \geq 0 \quad (6)$$

where p denotes the pdf, $\Omega_p = E[\alpha^2]$ is the average signal power, K is the Ricean factor, x is the value of the signal envelope, and I_0 is the modified Bessel function of the first kind and zero order. Similarly, the Nakagami distribution [6] is used to describe the distribution of the narrowband received signal envelope [25, pp. 53–55], which is given by

$$p_{\alpha}(x) = \frac{2m^m x^{2m-1}}{\Gamma(m)\Omega_p^m} \exp\left(-\frac{mx^2}{\Omega_p}\right), \quad m \geq \frac{1}{2} \quad (7)$$

where m is the Nakagami shape factor, and Γ is the Gamma function. Both distributions are related by the following approximate relationship between the Ricean factor and the Nakagami shape factor [25, pp. 54]

$$m \approx \frac{(K+1)^2}{(2K+1)}. \quad (8)$$

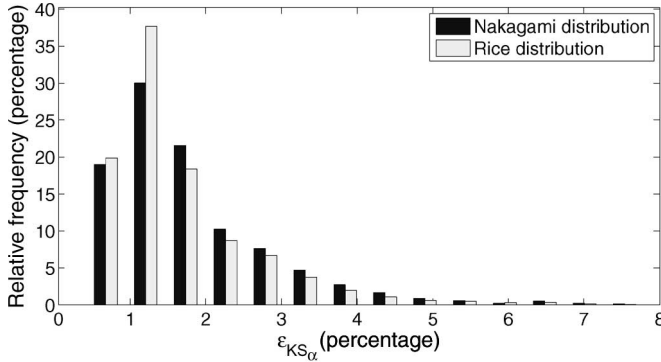


Fig. 1. Distribution of ϵ_{KS_α} .

TABLE II
ERROR STATISTICS IN THE APPROXIMATION OF THE DISTRIBUTION OF THE WIDEBAND SIGNAL ENVELOPE USING THE RICE AND NAKAGAMI DISTRIBUTIONS

	Nakagami distribution	Rice distribution
Mean ϵ_{KS_α}	1.78%	1.65%
Mean ϵ_{rms_α}	0.91%	0.85%
95th Percentile ϵ_{KS_α}	3.87%	3.58%
95th Percentile ϵ_{rms_α}	2.13%	2.01%
Max. ϵ_{KS_α}	7.80%	7.61%
Max. ϵ_{rms_α}	4.33%	4.30%

As a first step in our evaluation, we test over how many configurations the fading signal envelope is a strict realization of the Rice/Nakagami distributions. The KS test, which is set at a significance level of 5% (Type I error), indicates a strict realization of the Rice and Nakagami distributions in 50.53% and 43.89% of the configurations, respectively. To establish the practical relevance of these figures, further investigation is required [26, pp. 529–530]. This is done by analyzing the error statistics.

Fig. 1 shows a histogram of ϵ_{KS_α} , which is the maximum difference between the empirical and proposed cdf of the signal envelope for each configuration. ϵ_{KS_α} is less than 7.8% for all configurations, and its values lie mostly in the range 0.5%–2% for both the Rice and Nakagami distributions. It is noted that, by this measure, the Rice distribution is a somewhat better approximation to the EDF than is the Nakagami distribution but that the difference is marginal. The distribution of ϵ_{rms_α} is very similar to that of ϵ_{KS_α} (see Table II), tallying with the latter statement.

The numerical results are summarized in Table II. The average ϵ_{KS_α} over all configurations is 1.65% and 1.78% for the Rice and Nakagami distributions, respectively. The 95th percentile of ϵ_{KS_α} is less than 3.9% for both distributions, underlining the overall goodness-of-fit. The largest ϵ_{KS_α} observed for a configuration is 7.8% using the Nakagami distribution. Again, the Rice distribution fares slightly better by this measure. However, since the observed differences in goodness-of-fit between both distributions are marginal, we conclude that the Rice and Nakagami distributions are practically equally well suited to characterize the wideband fading signal envelope over the range of parameters chosen.

Important observations can be made about the ability of the Rice/Nakagami distribution to characterize the distribution of the wideband signal envelope by evaluating the dependence of

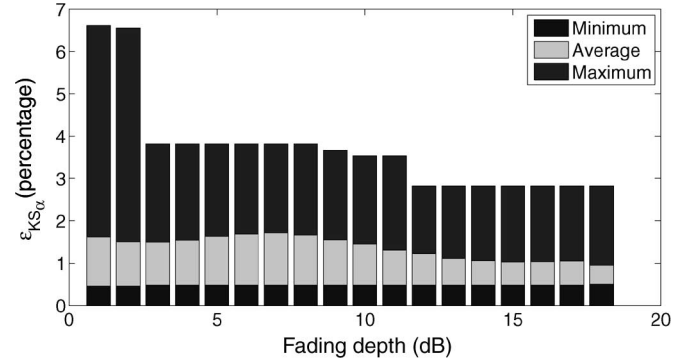


Fig. 2. Dependence of ϵ_{KS_α} on the fading depth.

the approximation error on the fading depth. The fading depth is taken to be the difference between the signal levels that correspond to 50% and 1% of the cdf. In Fig. 2, the variation of ϵ_{KS_α} with a fading depth is shown for the Rice distribution. First, we observe that the minimum ϵ_{KS_α} is virtually independent of the fading depth. Second, the average ϵ_{KS_α} tends to be greater for a shallower fading depth but starts to decrease for fading depths greater than about 8 dB and levels off for fading depths greater than about 13 dB. The maximum ϵ_{KS_α} shows a sharp rise for fading depths less than 3 dB. These latter two observations indicate that the approximation gets better with greater fading depths. This is desirable since the stronger the fading, the more important an accurate description of the phenomenon is. However, it also shows the limitation of characterizing wideband fading signals by Rice/Nakagami distributions. Where there are small fading depths (< 3 dB), the approximation is still good on the average; however, sporadically higher approximation errors can be observed. Since the fading depth increases with a decreasing maximum difference in propagation path lengths ΔL_{max} , we expect the approximation of the distribution of the wideband signal envelope by the Rice/Nakagami distributions to apply somewhat better in microcellular environments than in macrocellular environments where ΔL_{max} is typically greater.

Where the Rice distribution describes signal envelope fading, the distribution of the signal power is described by the noncentral chi-square distribution with two degrees of freedom [25, pp. 51–53] as

$$p_{\alpha^2}(x) = \frac{K+1}{\Omega_p} \exp\left(-K - \frac{(K+1)x}{\Omega_p}\right) \times I_0\left(2\sqrt{\frac{K(K+1)x}{\Omega_p}}\right), \quad x \geq 0. \quad (9)$$

Likewise, if the Nakagami distribution describes signal envelope fading, then the distribution of the signal power follows the Gamma distribution [25, pp. 53–55], which is expressed as

$$p_{\alpha^2}(x) = \left(\frac{m}{\Omega_p}\right)^m \frac{x^{m-1}}{\Gamma(m)} \exp\left(-\frac{mx}{\Omega_p}\right), \quad m \geq \frac{1}{2}. \quad (10)$$

Employing the same method used for the signal envelope, we determined that the power distribution can be characterized by the noncentral chi-square/Gamma distributions to a similar degree of accuracy as the signal envelope is characterized by

TABLE III
SYSTEM BANDWIDTHS OF VARIOUS WIRELESS STANDARDS

Wireless standard	System bandwidth (MHz)
UMTS	3.38 [41]
DSRC	8.13 [42]
802.11, 802.11b	9.68 [43, pp. 195]
WiMAX (Europe)	14 [44]
802.11a, HIPERLAN Type II	16.56 [45]

the Rice/Nakagami distributions. The difference in accuracy is $\ll 10^{-2}\%$ by all measures used in Table II.

III. MAPPING WIDEBAND PROPAGATION PARAMETERS TO THE RICEAN K -FACTOR AND THE NAKAGAMI SHAPE FACTOR

In the previous section, it was shown that wideband signal envelope fading can be characterized to a good approximation by the Rice and Nakagami distributions in urban microcells. In this section, we obtain an approximate functional relationship between the wideband fading parameters ($2\Delta f$, ΔL_{\max} , a (dB)) and the Ricean K -factor using a curve-fitting approach. That is

$$F_k : \mathcal{S}_{2\Delta f} \times \mathcal{S}_{\Delta L_{\max}} \times \mathcal{S}_a \rightarrow \mathcal{S}_K, \quad \mathcal{S}_K \in \mathbb{R}. \quad (11)$$

This is done for a number of different wireless standards. The accuracy of this approach is then assessed. The Ricean factor K is determined by MLE over a discrete range of wideband propagation parameters, as described in Section II, and the results are tabulated. F_k is then determined by fitting an appropriate function to the value table. In the early stages of the curve-fitting process, we observed that no one function describes this mapping to a high degree of accuracy for all configurations. However, by fixing the bandwidth, we obtain individual functions that fit the value table for the various wireless standards. The mapping is performed in a linear instead of a logarithmic space so that the problem of mapping a value of $-\infty$ dB for the NLOS case is circumvented. The 3-dB bandwidths of some of the widely used wireless standards are displayed in Table III. The bandwidths of DSSS-based systems are calculated using [27, p. 21]; the bandwidth of orthogonal frequency-division multiplexing-based systems is calculated using [28, pp. 43, eq. (2.35)].

We use the following procedure to obtain the functional relationship F_k for the wireless standards given in Table III, which can also be used to derive mappings for other wireless standards.

- 1) Determine a value table for the wireless standard under consideration containing the wideband propagation parameters ΔL_{\max} , a , and the Ricean factor K that is determined by MLE, as described in Section II.
- 2) Choose a candidate function for curve fitting. If this function requires the wideband propagation parameters to lie within a specified range, as exemplified for the Chebyshev polynomial series, then the parameters must be scaled to that range.
- 3) Estimate the constants in the candidate function by minimizing the approximation error between the Ricean

factor K obtained in step 1), and the approximate value of K as given by the candidate function.

- 4) Calculate the mean, the 95th percentile, and the maximum ε_{KS} for the approximation function that was determined in step 3).
- 5) If the error statistics in step 4) are satisfactory, terminate. Otherwise, go back to step 2).

The Chebyshev polynomial series is well known to be suitable for curve-fitting purposes. Its advantage lies in the fact that if the series is truncated to a polynomial of a lower degree, the consequent degradation in accuracy is graceful [29, pp. 190–194]. We found, by using the above procedure, that the following eighth-degree Chebyshev polynomial approximates the Ricean factor K well for all standards:

$$F_k(a, \Delta L_{\max}) = c_{0,0} + \sum_{i=1}^7 \sum_{j=1}^i c_{i,j} T_{8-i}(x) T_j(y) + \sum_{i=1}^8 (c_{8,i} T_i(x) + c_{9,i} T_i(y)) \quad (12)$$

where

$$T_n(z) = \cos(n \arccos(z)) \quad (13)$$

$$x = \frac{a}{15.8115} - 1 \quad (14)$$

$$y = \frac{\Delta L_{\max} - 0.1}{27.45} - 1 \quad (15)$$

and the constants are given in Tables V and VI in the Appendix. The Chebyshev polynomials require that their input parameters are in the range $[-1, 1]$ [29, pp. 191–192], which is achieved via (14) and (15).

The goodness-of-fit of the Rice distribution, where K has been obtained using the approximation function F_k in describing the distribution of the small-scale fading wideband signal envelope, is displayed in Table IV. It can be observed that the low average $\varepsilon_{\text{KS}_\alpha}$ values indicate a very good fit. As in Section II, we observe that the maximum values tend to increase with a shallower fading depth. There is up to a 0.5% difference in $\text{Max}\varepsilon_{\text{KS}_\alpha}$ introduced due to the function approximation for K .

The relationship between the wideband propagation parameters ΔL_{\max} , a , and the Ricean factor K is illustrated in Fig. 3 by graphing F_k for the IEEE 802.11 standard. The Ricean factor K has, for very small values of ΔL_{\max} , a value equal to a . The reason for this is that small-scale fading in such propagation environments is equally severe for wideband and narrowband signals; this phenomenon has also been reported by Yan and Kozono [1]. However, such small values of ΔL_{\max} are rarely observed in microcells. As ΔL_{\max} increases, the small-scale fading becomes less severe—as also observed by Yan and Kozono [1]—and consequently, the Ricean factor K increases. This increase is magnified for greater values of a .

TABLE IV
ERROR STATISTICS IN THE GOODNESS-OF-FIT OF THE RICE DISTRIBUTION TO THE EDF, WHERE K HAS BEEN OBTAINED VIA F_k

Wireless standard	Mean $\varepsilon_{KS,\alpha}$	95th Percentile $\varepsilon_{KS,\alpha}$	Max. $\varepsilon_{KS,\alpha}$
UMTS	1.74%	3.12%	3.89%
DSRC	1.66%	2.99%	4.81%
802.11, 802.11b	1.64%	3.05%	4.45%
WiMAX (Europe)	2.13%	4.56%	6.19%
802.11a,	2.36%	5.56%	7.70%
HIPERLAN T. II			

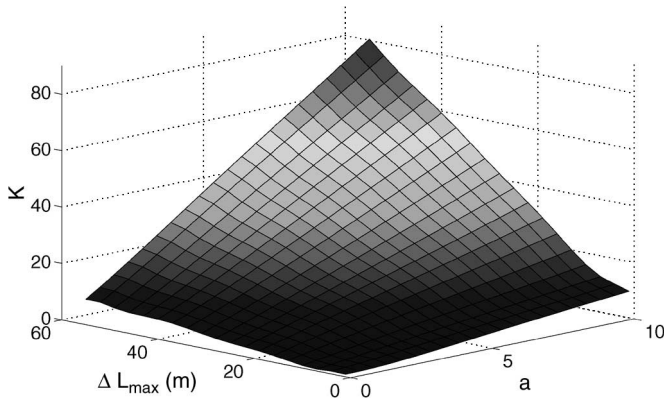


Fig. 3. Relation between the wideband propagation parameters ΔL_{max} , a , and the Ricean factor K for the IEEE 802.11 standard.

IV. APPLICATIONS

We begin this section by outlining the steps that are necessary to adapt commonly used equations and solutions for small-scale signal/power envelope fading for narrowband systems to wideband systems. We then apply the results of this paper to derive the appropriate window size for local mean power estimation in IEEE 802.11 systems. We conclude this section with two applications: the computationally efficient simulation of small-scale wideband signal envelope fading for a packet-level wireless network simulator and the derivation of a BEP model for an ideal IEEE 802.11 receiver.

The stochastic process of small-scale signal envelope fading for narrowband and wideband systems is described by its pdfs and autocorrelation function. We have shown in this paper that the same pdfs characterize small-scale signal envelope fading in narrowband and wideband systems in microcells, albeit with different parameters for which we provide a mapping between the two. These results allow, together with Nakabayashi and Kozono’s [18] result that the autocorrelation of small-scale signal envelope fading is independent of the bandwidth, adaptation of narrowband solutions for small-scale signal/power envelope fading to wideband solutions for microcells. The following steps are necessary for such adaptation.

- 1) Verify that the narrowband solution is independent of assumptions or properties that differ from those for the given wideband channel. For example, the BEP function of a receiver with a given decoding scheme might be modeled for a small-scale fading narrowband channel described by the Rice distribution. However, the performance of such a receiver is typically derived under the assumption that no intersymbol interference exists. However, intersymbol interference is common in wideband channels [30, pp. 235–239]. Consequently, such

a BEP function, depending on the small-scale narrowband signal envelope fading, can only be adapted to a receiver in wideband channels if the existence of a perfect channel equalizer is assumed [30, pp. 248, 343], [31, pp. 355–357].

- 2) Replace the Ricean factor K in the narrowband solution with F_k (12) using the constants from Tables V and VI for the wireless standard in question. If the narrowband solution depends on the Nakagami shape factor m , then one must first map m to K via (8) and then use F_k . If the mapping for the wireless standard in question is not given in this paper, it can be obtained as outlined in Section III.

A. Estimation of the Local Mean Power in IEEE 802.11 Systems

Accurate estimation of the local mean power at a receiver is essential in handover algorithms in cellular networks. The method that is widely used for this task (signal power averaging over an appropriately chosen distance with appropriate sample spacing) originated from Lee [32] and was later extended by Austin and Stueber [33] for the Rice distribution. We first summarize some of Austin and Stueber’s [25, pp. 598–605] [33] results for narrowband systems and then extend these results for an IEEE 802.11 system in an urban street with a maximum cell radius of 250 m. The received signal power is given by [33, eq. (5)]

$$\alpha_r^2(y) = \alpha^2(y) \cdot \Omega_p(y) \tag{16}$$

where $\alpha^2(y)$ is the power of the small-scale fading signal, and $\Omega_p(y)$ is the local mean power. In the regions where the local mean is constant, the accuracy of the estimate can be expressed by the 1σ spread [33, eq. (10)], which is given by

$$1\sigma \text{ spread} = 10 \log_{10} \frac{\Omega_p + \sigma_{\Omega_p}}{\Omega_p - \sigma_{\Omega_p}} \tag{17}$$

where σ_{Ω_p} is the standard deviation of the estimated local mean power Ω_p . For analog averaging, $\sigma_{\Omega_p}^2$ is given by [33, eq. (9)]

$$\begin{aligned} \sigma_{\Omega_p}^2 = & \left(\frac{\Omega_p}{K+1} \right)^2 \frac{1}{G} \\ & \times \int_0^{2G} \left(1 - \frac{g}{2G} \right) I_0 \left(\frac{2\pi g}{\lambda_c} \right) \\ & \times \left(I_0 \left(\frac{2\pi g}{\lambda_c} \right) + 2K \cos \left(\frac{2\pi g \cos(\theta_0)}{\lambda_c} \right) \right) dg \end{aligned} \tag{18}$$

TABLE V
CONSTANTS OF (12), PART I

Constant	UMTS	DSRC	802.11, 802.11b
$c_{0,0}$	$2.65638 \cdot 10^1$	$5.73860 \cdot 10^1$	$6.59047 \cdot 10^1$
$c_{1,1}$	$1.37812 \cdot 10^1$	$4.23944 \cdot 10^1$	$5.26263 \cdot 10^1$
$c_{1,2}$	$2.86887 \cdot 10^0$	$2.20801 \cdot 10^0$	$2.68786 \cdot 10^0$
$c_{1,3}$	$-7.25628 \cdot 10^{-1}$	$-2.68774 \cdot 10^0$	$-2.07149 \cdot 10^0$
$c_{1,4}$	$-5.55885 \cdot 10^{-1}$	$7.24910 \cdot 10^{-1}$	$1.28425 \cdot 10^0$
$c_{1,5}$	$-5.08939 \cdot 10^{-2}$	$-2.74460 \cdot 10^{-1}$	$-5.48678 \cdot 10^{-1}$
$c_{1,6}$	$4.94091 \cdot 10^{-2}$	$1.14778 \cdot 10^{-1}$	$6.47051 \cdot 10^{-2}$
$c_{1,7}$	$2.51037 \cdot 10^{-1}$	$7.59186 \cdot 10^{-1}$	$4.26026 \cdot 10^{-1}$
$c_{2,1}$	$-3.28653 \cdot 10^{-1}$	$1.62175 \cdot 10^{-1}$	$7.30515 \cdot 10^{-1}$
$c_{2,2}$	$-1.72785 \cdot 10^{-1}$	$-1.15478 \cdot 10^{-1}$	$3.74852 \cdot 10^{-2}$
$c_{2,3}$	$-3.11678 \cdot 10^{-1}$	$-1.84657 \cdot 10^{-1}$	$-2.16077 \cdot 10^{-1}$
$c_{2,4}$	$-3.57024 \cdot 10^{-2}$	$1.21763 \cdot 10^{-1}$	$-1.55779 \cdot 10^{-1}$
$c_{2,5}$	$-1.88604 \cdot 10^{-2}$	$-1.40336 \cdot 10^{-1}$	$-3.45822 \cdot 10^{-1}$
$c_{2,6}$	$2.50330 \cdot 10^{-1}$	$-9.47594 \cdot 10^{-2}$	$-1.81959 \cdot 10^{-2}$
$c_{3,1}$	$-1.48940 \cdot 10^{-1}$	$2.45746 \cdot 10^{-1}$	$3.78772 \cdot 10^{-1}$
$c_{3,2}$	$-1.42424 \cdot 10^{-1}$	$-2.70189 \cdot 10^{-2}$	$-2.57752 \cdot 10^{-2}$
$c_{3,3}$	$1.26737 \cdot 10^{-2}$	$-7.43703 \cdot 10^{-2}$	$8.94587 \cdot 10^{-2}$
$c_{3,4}$	$8.78986 \cdot 10^{-2}$	$-3.30148 \cdot 10^{-1}$	$-7.63737 \cdot 10^{-2}$
$c_{3,5}$	$1.34503 \cdot 10^{-1}$	$-3.09275 \cdot 10^{-1}$	$-1.95375 \cdot 10^{-1}$
$c_{4,1}$	$-4.86988 \cdot 10^{-2}$	$-1.30967 \cdot 10^{-1}$	$1.77666 \cdot 10^{-1}$
$c_{4,2}$	$3.94004 \cdot 10^{-2}$	$2.00451 \cdot 10^{-1}$	$2.17075 \cdot 10^{-1}$
$c_{4,3}$	$1.44729 \cdot 10^{-1}$	$-6.33639 \cdot 10^{-2}$	$1.83147 \cdot 10^{-1}$
$c_{4,4}$	$1.43865 \cdot 10^{-1}$	$-2.38714 \cdot 10^{-1}$	$1.52262 \cdot 10^{-1}$
$c_{5,1}$	$2.17622 \cdot 10^{-1}$	$-1.44119 \cdot 10^{-1}$	$-5.02657 \cdot 10^{-2}$
$c_{5,2}$	$9.43872 \cdot 10^{-3}$	$3.80796 \cdot 10^{-1}$	$4.36697 \cdot 10^{-1}$
$c_{5,3}$	$1.22688 \cdot 10^{-1}$	$1.42236 \cdot 10^{-1}$	$3.29747 \cdot 10^{-1}$
$c_{6,1}$	$2.66421 \cdot 10^{-1}$	$5.29977 \cdot 10^{-2}$	$-1.44150 \cdot 10^{-1}$
$c_{6,2}$	$6.35142 \cdot 10^{-2}$	$2.97995 \cdot 10^{-1}$	$3.39882 \cdot 10^{-1}$
$c_{7,1}$	$1.95478 \cdot 10^{-1}$	$5.41460 \cdot 10^{-2}$	$-1.37397 \cdot 10^{-1}$
$c_{8,1}$	$2.45464 \cdot 10^1$	$5.55525 \cdot 10^1$	$6.25894 \cdot 10^1$
$c_{8,2}$	$-9.70984 \cdot 10^{-1}$	$2.36040 \cdot 10^0$	$1.30470 \cdot 10^0$
$c_{8,3}$	$-3.47196 \cdot 10^{-1}$	$4.92801 \cdot 10^{-1}$	$3.67036 \cdot 10^{-1}$
$c_{8,4}$	$5.87212 \cdot 10^{-1}$	$-1.13974 \cdot 10^0$	$-7.74282 \cdot 10^{-2}$
$c_{8,5}$	$1.10683 \cdot 10^0$	$-2.43033 \cdot 10^0$	$-8.28685 \cdot 10^{-1}$
$c_{8,6}$	$1.36636 \cdot 10^0$	$-2.44872 \cdot 10^0$	$-9.42947 \cdot 10^{-1}$
$c_{8,7}$	$9.04447 \cdot 10^{-1}$	$-1.68777 \cdot 10^0$	$-6.69374 \cdot 10^{-1}$
$c_{8,8}$	$3.41023 \cdot 10^{-1}$	$-4.90294 \cdot 10^{-1}$	$-1.13625 \cdot 10^{-1}$
$c_{9,1}$	$1.54564 \cdot 10^1$	$4.59253 \cdot 10^1$	$5.66118 \cdot 10^1$
$c_{9,2}$	$3.06967 \cdot 10^0$	$2.27811 \cdot 10^0$	$2.76990 \cdot 10^0$
$c_{9,3}$	$-5.02265 \cdot 10^{-1}$	$-2.58672 \cdot 10^0$	$-1.93193 \cdot 10^0$
$c_{9,4}$	$-4.57437 \cdot 10^{-1}$	$5.98170 \cdot 10^{-1}$	$1.41196 \cdot 10^0$
$c_{9,5}$	$7.25653 \cdot 10^{-2}$	$-1.92815 \cdot 10^{-1}$	$-3.22624 \cdot 10^{-1}$
$c_{9,6}$	$-1.81167 \cdot 10^{-1}$	$1.12025 \cdot 10^{-1}$	$3.30403 \cdot 10^{-2}$
$c_{9,7}$	$2.40094 \cdot 10^{-1}$	$9.12304 \cdot 10^{-1}$	$4.47269 \cdot 10^{-1}$
$c_{9,8}$	$-1.66003 \cdot 10^{-1}$	$-6.86901 \cdot 10^{-2}$	$-3.36637 \cdot 10^{-1}$

TABLE VI
CONSTANTS OF (12), PART II

Constant	WiMAX	802.11a, HIPERLAN Type II
$c_{0,0}$	$8.76270 \cdot 10^1$	$1.13186 \cdot 10^2$
$c_{1,1}$	$7.48435 \cdot 10^1$	$9.38172 \cdot 10^1$
$c_{1,2}$	$1.81718 \cdot 10^0$	$9.27280 \cdot 10^{-1}$
$c_{1,3}$	$-2.56708 \cdot 10^0$	$-2.93542 \cdot 10^0$
$c_{1,4}$	$1.47843 \cdot 10^0$	$1.36397 \cdot 10^0$
$c_{1,5}$	$-8.57421 \cdot 10^{-1}$	$-1.20001 \cdot 10^0$
$c_{1,6}$	$1.98571 \cdot 10^{-1}$	$1.04618 \cdot 10^0$
$c_{1,7}$	$5.78706 \cdot 10^{-3}$	$3.93874 \cdot 10^{-1}$
$c_{2,1}$	$-2.20253 \cdot 10^0$	$1.15162 \cdot 10^0$
$c_{2,2}$	$-9.96457 \cdot 10^{-1}$	$6.37858 \cdot 10^{-2}$
$c_{2,3}$	$-1.06276 \cdot 10^0$	$-1.26930 \cdot 10^{-1}$
$c_{2,4}$	$-7.02574 \cdot 10^{-1}$	$4.46329 \cdot 10^{-2}$
$c_{2,5}$	$-6.53393 \cdot 10^{-1}$	$4.56496 \cdot 10^{-2}$
$c_{2,6}$	$-3.01985 \cdot 10^{-1}$	$5.04646 \cdot 10^{-1}$
$c_{3,1}$	$-1.10417 \cdot 10^0$	$3.14616 \cdot 10^{-1}$
$c_{3,2}$	$-9.16816 \cdot 10^{-1}$	$3.40990 \cdot 10^{-1}$
$c_{3,3}$	$-8.15853 \cdot 10^{-1}$	$1.24125 \cdot 10^{-1}$
$c_{3,4}$	$-5.66470 \cdot 10^{-1}$	$-2.44335 \cdot 10^{-1}$
$c_{3,5}$	$-3.76809 \cdot 10^{-1}$	$1.47865 \cdot 10^{-3}$
$c_{4,1}$	$4.80351 \cdot 10^{-1}$	$-7.77204 \cdot 10^{-1}$
$c_{4,2}$	$-2.30076 \cdot 10^{-1}$	$1.26390 \cdot 10^{-2}$
$c_{4,3}$	$-3.15561 \cdot 10^{-1}$	$-1.81383 \cdot 10^{-1}$
$c_{4,4}$	$3.35545 \cdot 10^{-2}$	$-4.05003 \cdot 10^{-1}$
$c_{5,1}$	$1.85959 \cdot 10^0$	$-1.36030 \cdot 10^0$
$c_{5,2}$	$1.96556 \cdot 10^{-1}$	$4.25680 \cdot 10^{-2}$
$c_{5,3}$	$2.83263 \cdot 10^{-2}$	$3.43354 \cdot 10^{-2}$
$c_{6,1}$	$2.15135 \cdot 10^0$	$-1.01214 \cdot 10^0$
$c_{6,2}$	$2.53135 \cdot 10^{-1}$	$2.33021 \cdot 10^{-1}$
$c_{7,1}$	$9.79141 \cdot 10^{-1}$	$-4.11092 \cdot 10^{-1}$
$c_{8,1}$	$7.87694 \cdot 10^1$	$1.10503 \cdot 10^2$
$c_{8,2}$	$-4.46444 \cdot 10^0$	$6.27350 \cdot 10^0$
$c_{8,3}$	$-1.48506 \cdot 10^0$	$1.07976 \cdot 10^0$
$c_{8,4}$	$2.05396 \cdot 10^0$	$-3.18989 \cdot 10^0$
$c_{8,5}$	$4.60730 \cdot 10^0$	$-6.66513 \cdot 10^0$
$c_{8,6}$	$5.27685 \cdot 10^0$	$-7.11342 \cdot 10^0$
$c_{8,7}$	$3.21195 \cdot 10^0$	$-4.59178 \cdot 10^0$
$c_{8,8}$	$8.92708 \cdot 10^{-1}$	$-1.27969 \cdot 10^0$
$c_{9,1}$	$8.23151 \cdot 10^1$	$1.00352 \cdot 10^2$
$c_{9,2}$	$2.30991 \cdot 10^0$	$1.21875 \cdot 10^0$
$c_{9,3}$	$-2.00708 \cdot 10^0$	$-2.64205 \cdot 10^0$
$c_{9,4}$	$1.81532 \cdot 10^0$	$1.25771 \cdot 10^0$
$c_{9,5}$	$-4.95736 \cdot 10^{-1}$	$-1.18167 \cdot 10^0$
$c_{9,6}$	$3.81488 \cdot 10^{-1}$	$5.99549 \cdot 10^{-1}$
$c_{9,7}$	$1.46104 \cdot 10^{-1}$	$3.43866 \cdot 10^{-2}$
$c_{9,8}$	$-8.67049 \cdot 10^{-2}$	$-3.38656 \cdot 10^{-1}$

and for digital averaging, it is given by [33, eq. (14)]

$$\sigma_{\Omega_p}^2 = \left(\frac{\Omega_p}{K+1} \right)^2 \left(\frac{1+2K}{N} + 2 \sum_{n=1}^{N-1} \left(\frac{N-n}{N^2} \right) \cdot I_0 \left(\frac{2\pi ns}{\lambda_c} \right) \right. \\ \left. \times \left(I_0 \left(\frac{2\pi ns}{\lambda_c} \right) + 2K \cos \left(\frac{2\pi ns \cos(\theta_0)}{\lambda_c} \right) \right) \right) \quad (19)$$

where G is the ‘‘window size’’ or the distance over which the averaging is performed (measured in wavelengths), N is the number of samples taken over the interval, I_0 is the zero-order Bessel function of the first kind, λ_c is the carrier wavelength, θ_0 is the angle between the vector in the direction of propagation of the direct wave and the velocity of the receiver, and ‘‘ s ’’ is the sample spacing (measured in wavelengths).

The derivation of (18) and (19) only requires knowledge of the pdf and autocorrelation of the small-scale fading signal envelope. We have shown how to obtain a reliable estimate for the former for wideband signals, whereas the latter has been shown to be bandwidth independent [18], and therefore, these equations will apply to wideband systems where the appropriate value of K is used, as has been described in this paper.

The adaptation to an IEEE 802.11 system is straightforward. Only the Ricean factor K has to be determined, as described above via the function $F_k(a; \Delta L_{\max})$. The range of ΔL_{\max} is determined by the network type and the street geometry. We choose 250 m as the maximum cell range, corresponding to our own measurements for an IEEE 802.11 network [11]. Fig. 4 shows the variation in the 1σ spread with ΔL_{\max} and G for analog averaging in NLOS conditions. The 1σ spread

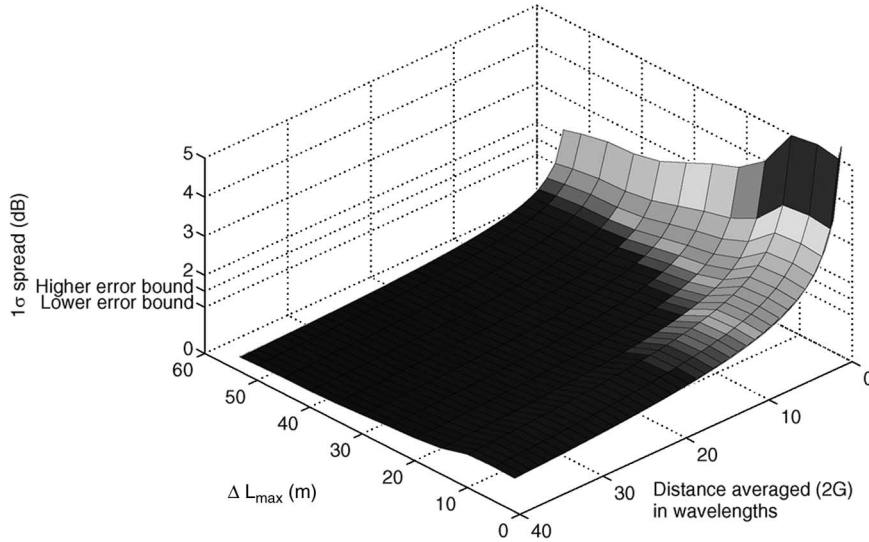


Fig. 4. The 1σ spread in the NLOS condition, depending on the averaging distance and ΔL_{\max} .

values, which correspond to a window size of $20\lambda_c$ and $40\lambda_c$, as suggested by Lee for narrowband systems, have been marked on the z -axis as “higher error bound” and “lower error bound,” respectively. Compared to the classical narrowband case, in which the result is independent of the maximum difference in propagation path lengths ΔL_{\max} , it is clear that $\sigma_{\Omega_p}^2$ strongly depends on ΔL_{\max} . However, for the propagation environment under consideration, an averaging window size of between $13\lambda_c$ and $25\lambda_c$ guarantees to be within the desired error bounds. Since the autocorrelation function is bandwidth independent, it follows from Stueber [25, pp. 603–604] that the sample spacing should be less than $0.5\lambda_c$ for wideband systems as well.

B. Simulation of Wideband Small-Scale Signal Envelope Fading for an IEEE 802.11 System

The open-source packet-level simulator NS-2 [34] is the most popular simulator in the mobile *ad hoc* network community [35]. The simulator ships without any support for the simulation of small-scale fading, although such a module exists from Punnoose *et al.* [36]. This module simulates small-scale signal envelope fading using the Rice distribution and is applied for narrowband channels only. The module is computationally very efficient because it uses a precomputed lookup table for the otherwise costly generation of correlated signal envelope samples for each packet.

Punnoose *et al.*'s module is based solely on the Rice distribution and the bandwidth-independent autocorrelation of the small-scale fading signal envelope and is not based on any other assumptions that may be different for wideband systems. This module is adapted to simulate small-scale signal envelope fading for an IEEE 802.11 system in microcells by simply replacing the Ricean factor K with F_k , where F_k is given by (12) using the constants from Table V for an IEEE 802.11 system.

The simulation of an IEEE 802.11 system requires that the performance of the receiver, which is typically expressed by its average BEP, is correctly modeled. The average BEP for

an ideal IEEE 802.11 receiver with DQPSK for 2 Mb/s can be obtained from a narrowband BEP model using the methods outlined in this paper. The average BEP \bar{P}_b for an IEEE 802.11 receiver with coherent DQPSK modulation for a Ricean fading narrowband channel can be modeled as [37, p. 188, eq. (6.70)], [37, p. 187, eq. (6.64)]

$$\bar{P}_b(\bar{\gamma}_b, K) = \frac{1}{2} \frac{1 + K}{1 + K + \bar{\gamma}_b} \exp\left(\frac{-K\bar{\gamma}_b}{1 + K + \bar{\gamma}_b}\right) \quad (20)$$

where $\bar{\gamma}_b$ is the average signal-to-noise ratio, and K is the Ricean factor. As noted previously, this model can only be adapted for wideband channels in which no intersymbol interference is present, as would be the case where there is perfect channel equalization. Replacing the Ricean factor K with F_k for an IEEE 802.11 system gives

$$\bar{P}_b(\bar{\gamma}_b, a, \Delta L_{\max}) = \frac{1}{2} \frac{1 + F_k(a, \Delta L_{\max})}{1 + F_k(a, \Delta L_{\max}) + \bar{\gamma}_b} \cdot \exp\left(\frac{-F_k(a, \Delta L_{\max})\bar{\gamma}_b}{1 + F_k(a, \Delta L_{\max}) + \bar{\gamma}_b}\right) \quad (21)$$

which is the average BEP of an ideal IEEE 802.11 receiver with perfect equalization.

To show the effects of modeling the small-scale signal fading as wideband over narrowband, we conducted two simulations using the NS-2 simulator for an IEEE 802.11 system, as described above. These simulations were performed using two nodes where the transmitter was stationary and the receiver was moving away with a constant velocity. The variations in the signal power are due only to small-scale fading. The receiver noise floor was set to -104 dBm, which is a typical value for an IEEE 802.11 receiver [38]. Both simulations were conducted for NLOS conditions for both narrowband and wideband channels. In the latter case, ΔL_{\max} was set to 40 m. The small-scale fading signal power is given for both simulations in Fig. 5. When the channel was modeled as being narrowband, the small-scale fading was severe and showed deep fades. In the case where the channel was modeled as

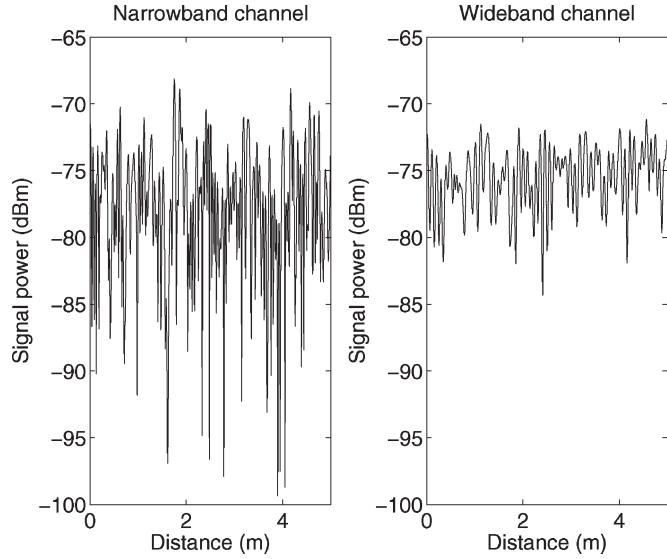


Fig. 5. Examples of small-scale signal power fading over distance for narrowband and wideband channels.

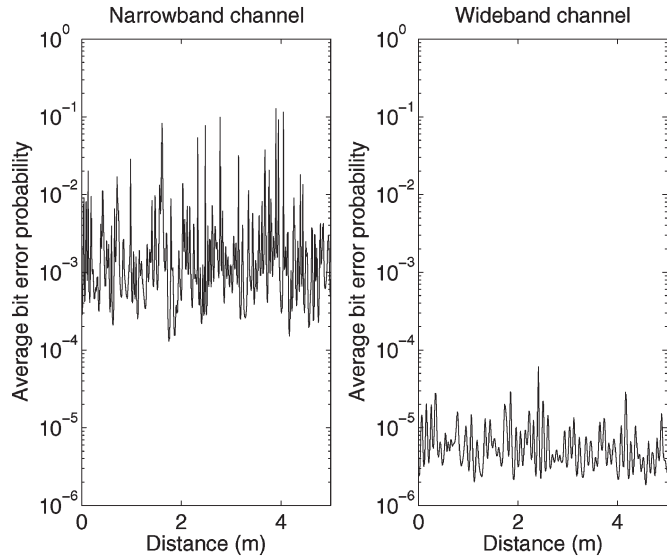


Fig. 6. Examples of the average BEP for an ideal IEEE 802.11 receiver over distance for narrowband and wideband channels.

wideband ($K = F_k$), the small-scale fading was significantly reduced. Fig. 6 shows the average BEP for an IEEE 802.11 receiver in the corresponding simulations of the narrowband and wideband channels. As expected, the average BER is considerably lower in the wideband channel. This difference is the result of less severe fading in the signal power and the modified BEP model.

V. CONCLUSION

This paper has shown that the distribution of the small-scale fading wideband signal envelope can be characterized by the Rice and Nakagami distributions and that the signal power is equally well characterized by the noncentral chi-square/Gamma distributions for microcells. It should be noted that the results in this paper apply also to picocells (since ΔL_{\max} is smaller).

We have shown how our results can be used to determine the appropriate window size when estimating the local mean power in a wideband system and that the window size is typically smaller than that used for narrowband systems.

Packet-level wireless network simulation software such as NS-2 is widely used but is currently restricted because it models the fading distribution of the wideband signal envelope using narrowband techniques. We have shown how the NS-2 simulator, which models small-scale signal envelope fading using the module of Punnoose *et al.* [39], can be adapted for wideband systems. Moreover, we demonstrated that a BEP model for DQPSK receivers in narrowband channels can be used to model IEEE 802.11 receivers with perfect channel equalization. We have illustrated in simulations that an IEEE 802.11 system performs considerably better when small-scale signal envelope fading is modeled as wideband over narrowband.

Although normally based on the large-scale fading phenomenon, our recent study of link quality prediction for IEEE 802.11 in urban microcells indicates that the accurate prediction of link quality (i.e., outage probability) would benefit where large-scale fading is also considered [11]. However, such outage probability calculations require an accurate description of the cdf of the signal envelope, which can be done using the Rice and Nakagami distributions with the appropriate values of K and m , respectively, as this paper has shown, thus enabling such calculations for wideband systems.

APPENDIX

DEFINITIONS OF DISTRIBUTION FUNCTIONS

Let $\text{Prob}[\cdot]$ denote the probability of the given argument. The definitions for the pdf, cdf, and EDF are then given as follows.

Definition 1 (pdf): The pdf of a continuous random variable X is a real-valued function $p(x)$ such that [40, eq. (3.25)]

$$\text{Prob}[b \leq X \leq d] = \int_b^d p(x)dx, \quad b, d \in \mathbb{R}, \quad b \leq d.$$

Definition 2 (cdf): The cdf $P_{\text{cdf}}(x)$ for a continuous random variable X is defined by [40, eq. (3.26)]

$$P_{\text{cdf}}(x) = \text{Prob}[X \leq x] = \int_{-\infty}^x p(y)dy, \quad -\infty < x < \infty. \quad (22)$$

Definition 3 (EDF): Suppose a sample of size n is drawn from a population with known cdf $P_{\text{cdf}}(x)$. The EDF $P_{\text{EDF}}(x)$ is defined by the sample and is a step function given by [40, eq. (14.2)]

$$P_{\text{EDF}}(x) = \frac{k}{n} \text{ when } x_{(i)} \leq x < x_{(i+1)} \quad (23)$$

where k is the number of observations that are less than or equal to x , and $\{x_{(i)}\}$ represents the order statistics. If the sample is drawn from the hypothesized distribution, then the EDF $P_{\text{EDF}}(x)$ should be close to $P_{\text{cdf}}(x)$.

REFERENCES

- [1] J. Yan and S. Kozono, "A study of received signal-level distribution in wideband transmissions in mobile communications," *IEEE Trans. Veh. Technol.*, vol. 48, no. 5, pp. 1718–1725, Sep. 1999.
- [2] W. C. Y. Lee, "Theory of wideband radio propagation," in *Proc. IEEE Veh. Technol. Conf.*, St. Louis, MO, 1991, pp. 285–288.
- [3] S. Kozono, "Received signal-level characteristics in a wide-band mobile radio channel," *IEEE Trans. Veh. Technol.*, vol. 43, no. 3, pp. 480–486, Aug. 1994.
- [4] A. Yamaguchi, K. Suwa, and R. Kawasaki, "Received signal level characteristics for wideband radio channel in microcells," in *Proc. Int. Symp. Pers., Indoor, Mobile Radio Commun.*, Toronto, ON, Canada, 1995, p. 1367.
- [5] W. R. Young, Jr., "Comparison of mobile radio transmission at 150, 450, 900, and 3700 MC," *Bell Syst. Tech. J.*, vol. 31, no. 6, pp. 1068–1085, 1952.
- [6] M. Nakagami, "The M-Distribution; A general formula of intensity of rapid fading," in *Proc. Symp. Statistical Methods Radio Wave Propag.*, W. G. Hoffman, Ed., W. G. Hoffman, Ed., 1960, pp. 3–36.
- [7] W. C. Jakes, Jr. and D. Reudink, "Comparison of mobile radio transmission at UHF and X-band," *IEEE Trans. Veh. Technol.*, vol. VT-16, no. 1, pp. 10–14, Oct. 1967.
- [8] R. H. Clarke, "Statistical theory of mobile-radio reception," *Bell Syst. Tech. J.*, vol. 47, no. 6, pp. 957–1000, 1968.
- [9] H. Suzuki, "A statistical model for urban radio propagation," *IEEE Trans. Commun.*, vol. COM-25, no. 7, pp. 673–680, Jul. 1977.
- [10] D. Oh, G. Lee, D. Choi, and C. Kim, "Statistical model of W-CDMA signals over realistic multipath channel," in *Proc. Veh. Technol. Conf.*, Rhodes, Greece, 2001, vol. 1, pp. 347–351.
- [11] G. Gaertner, E. O. Nuallain, A. Butterly, K. Singh, and V. Cahill, "802.11 link quality and its prediction—An experimental study," in *Personal Wireless Communications*, Lecture Notes in Computer Science, vol. 3260, Delft, The Netherlands: Springer-Verlag, 2004, pp. 147–163.
- [12] G. L. Turin, F. D. Clapp, T. L. Johnston, S. B. Fine, and D. Lavry, "A statistical model of urban multipath propagation," *IEEE Trans. Veh. Technol.*, vol. VT-21, no. 1, pp. 1–9, Feb. 1972.
- [13] H. Hashemi, "Simulation of the urban radio propagation channel," *IEEE Trans. Veh. Technol.*, vol. VT-28, no. 3, pp. 213–225, Aug. 1979.
- [14] "Proposal on channel transfer functions to be used in GSM late 1986," COST 207 WG1, CEPT, Paris, France, Tech. Rep., Sep. 1986.
- [15] A. Turkmani, D. Demery, and J. Parsons, "Measurement and modelling of wideband mobile radio channels at 900 MHz," *Proc. Inst. Electr. Eng. 1—Communications, Speech Vision*, vol. 138, no. 5, pp. 447–457, Oct. 1991.
- [16] W. Mohr, "Modeling of wideband mobile radio channels based on propagation measurements," in *Proc. IEEE Int. Symp. Pers., Indoor, Mobile Radio Commun.*, Toronto, ON, Canada, 1995, vol. 2, pp. 397–401.
- [17] D. Middleton, "Man-made noise in urban environments and transportation systems: Models and measurements," *IEEE Trans. Commun.*, vol. COM-21, no. 11, pp. 1232–1241, Nov. 1973.
- [18] H. Nakabayashi and S. Kozono, "Autocorrelation characteristics for received signal-level in a wide-band mobile radio channel," *Trans. IEICE*, vol. J81-B-II, no. 2, pp. 155–161, 1998.
- [19] H. Nakabayashi, J. Yan, H. Masui, M. Ishii, K. Sakawa, H. Shimizu, T. Kobayashi, and S. Kozono, "Validation of equivalent received bandwidth to characterize received signal level distribution through experiment and simulation," *IEICE Trans. Commun.*, vol. E84-B, no. 9, pp. 2550–2559, 2001.
- [20] F. D. Cardoso and L. M. Correia, "Fading depth dependence on system bandwidth in mobile communications—An analytical approximation," *IEEE Trans. Veh. Technol.*, vol. 52, no. 3, pp. 587–594, May 2003.
- [21] E. Green, "Radio link design for microcellular systems," *Brit. Telecom Technol. J.*, vol. 8, no. 1, pp. 85–96, 1990.
- [22] S. Kotz and N. Johnson, *Encyclopedia of Statistical Science*. Hoboken, NJ: Wiley, 1981.
- [23] J. Lagarias, J. A. Reeds, M. H. Wright, and P. E. Wright, "Convergence properties of the Nelder–Mead simplex method in low dimensions," *SIAM J. Optim.*, vol. 9, no. 1, pp. 112–147, 1998.
- [24] S. Rice, "Statistical properties of a sine wave plus noise," *Bell Syst. Tech. J.*, vol. 27, no. 1, pp. 109–157, 1948.
- [25] G. L. Stueber, *Principles of Mobile Communication*, 2nd ed. Norwell, MA: Kluwer, 2001.
- [26] M. DeGroot and M. Schervish, *Probability and Statistics*, 3rd ed. Reading, MA: Addison-Wesley, 2001.
- [27] R. C. Dixon, *Spread Spectrum Systems*, 2nd ed. Hoboken, NJ: Wiley, 1984.
- [28] M. R. D. Rodrigues, "Modelling and performance assessment of OFDM communication systems in the presence of non-linearities," Ph.D. dissertation, Univ. College London, London, U.K., 2002.
- [29] W. H. Press, B. P. Flannery, S. A. Teukolsky, and W. T. Vetterling, *Numerical Recipes in C: The Art of Scientific Computing*, 2nd ed. Cambridge, U.K.: Cambridge Univ. Press, 1992.
- [30] S. R. Saunders, *Antennas and Propagation for Wireless Communication Systems*, 1st ed. Hoboken, NJ: Wiley, 1999.
- [31] T. S. Rappaport, *Wireless Communications—Principles and Practice*, 2nd ed. Prentice Hall Communications Engineering and Emerging Technologies Series. Englewood Cliffs, NJ: Prentice-Hall, 2002.
- [32] W. C. Y. Lee, "Estimate of local average power of a mobile radio signal," *IEEE Trans. Veh. Technol.*, vol. VT-34, no. 1, pp. 22–27, Feb. 1985.
- [33] M. D. Austin and G. L. Stueber, "Velocity adaptive handoff algorithms for microcellular systems," *IEEE Trans. Veh. Technol.*, vol. 43, no. 3, pp. 549–561, Aug. 1994.
- [34] S. McCanne and S. Floyd, *NS-2 Network Simulator*, 2006. [Online]. Available: <http://www.isi.edu/nsnam/ns>
- [35] S. Kurkowski, T. Camp, and M. Colagrosso, "MANET simulation studies: The incredibles," *ACM SIGMOBILE Mobile Comput. Commun. Rev.*, vol. 9, no. 4, pp. 50–61, 2005.
- [36] R. J. Punnoose, P. V. Nikitin, and D. D. Stancil, "Efficient simulation of Ricean fading within a packet simulator," in *Proc. Veh. Technol. Conf.*, Tokyo, Japan, 2000, pp. 764–767.
- [37] A. Goldsmith, *Wireless Communications*, 1st ed. Cambridge, U.K.: Cambridge Univ. Press, 2005.
- [38] J. Zyren and A. Petrick, *Tutorial on Basic Link Budget Analysis—Application Note AN9804.1*, 1998.
- [39] R. J. Punnoose, P. V. Nikitin, J. Broch, and D. D. Stancil, "Optimizing wireless network protocols using real-time predictive propagation modeling," in *Proc. IEEE Radio Wireless Conf.*, Denver, CO, 1999, pp. 39–44.
- [40] D. Zwillinger and S. Kokoska, *CRC Standard Probability and Statistics Tables and Formulae*. Boca Raton, FL: CRC, 1999.
- [41] A. Sharma, "WCDMA and CDMA2000 compared," in *Proc. Wireless Commun. Netw. Conf.*, Orlando, FL, 2002, pp. 23–24.
- [42] J. Yin, G. Yeung, B. Ryu, S. Habermas, H. Krishnan, and T. Talty, "Performance evaluation of safety applications over DSRC vehicular ad hoc networks," in *Proc. ACM Workshop Veh. Ad Hoc Netw.*, Philadelphia, PA, 2004, pp. 1–9.
- [43] *International Standard ISO/IEC 8802-11: 1999(E)—Part 11: Wireless LAN Medium Access Control (MAC) and Physical Layer (PHY) Specifications*, 1999. Available: ANSI/IEEE Std. 802.11.
- [44] IEEE 802.16 WG, *System Parameters for 2–11 GHz Coexistence Simulations*, Tech. Rep., 2001.
- [45] R. van Nee, G. Awater, M. Morikura, M. Webster, and K. W. Halford, "New high-rate wireless LAN standards," *IEEE Commun. Mag.*, vol. 37, no. 12, pp. 82–88, Dec. 1999.



Gregor Gaertner received the Diploma (with distinction) in computer science from Ilmenau Technical University, Ilmenau, Germany, in 2001 and the Ph.D. degree from Trinity College Dublin, Dublin, Ireland, in 2007.

He is currently with the Distributed Systems Group, Department of Computer Science, Trinity College Dublin. His current research interests include wireless communications, mobile *ad hoc* networks, and distributed systems.



Eamonn O Nuallain received the degree in electrical engineering from University College Cork, Cork, Ireland in 1991 and the Ph.D. degree from Trinity College Dublin, Dublin, Ireland, in 2001.

He has worked with a number of blue-chip companies and currently lectures in telecommunications at Trinity College Dublin, where he is currently with the Distributed Systems Group, Department of Computer Science. His current research interests include mobile *ad hoc* networks, cognitive radio, channel modeling, and propagation.